Oncogene (2005) 24, 77–89

www.nature.com/onc

Manganese superoxide dismutase overexpression inhibits the growth of androgen-independent prostate cancer cells

Sujatha Venkataraman[1,2], Xiaohong Jiang[2], Christine Weydert[2], Yuping Zhang[2], Hannah J Zhang[2], Prabhat C Goswami[2,3], Justine M Ritchie[3], Larry W Oberley[2,3] and Garry R Buettner*[,1,2,3]

[1]*Free Radical and Radiation Biology Program – ESR Facility, University of Iowa, Iowa City, IA 52242-1101, USA;* [2]*Department of Radiation Oncology, University of Iowa, Iowa City, IA 52242-1101, USA;* [3]*Holden Comprehensive Cancer Center, University of Iowa, Iowa City, IA 52242-1101, USA*

This study investigates the role of the antioxidant enzyme manganese superoxide dismutase (MnSOD) in androgen-independent human prostate cancer (PC-3) cells' growth rate *in vitro* and *in vivo*. MnSOD levels were found to be lower in parental PC-3 cells compared to nonmalignant, immortalized human prostate epithelial cells (P69SV40T). To unravel the role of MnSOD in the prostate cancer phenotype, PC-3 cells were stably transfected with MnSOD cDNA plasmid. The MnSOD protein and activity levels in clones overexpressing MnSOD were increased seven- to eightfold. These cell lines showed elongated cell doubling time, reduced anchorage-independent growth in soft agar compared to parental PC-3 (Wt) cells, and reduced growth rate of PC-3 tumor xenografts in athymic nude mice. Flow cytometric studies showed an increase in membrane potential in the MnSOD-overexpressing clone (Mn32) compared to Wt and Neo cells. Also, production of extracellular H_2O_2 was increased in the MnSOD-overexpressing clones. As determined by DNA cell cycle analysis, the proportion of cells in G_1 phase was enhanced by MnSOD overexpression. Therefore, MnSOD not only regulates cell survival but also affects PC-3 cell proliferation by retarding G_1 to S transition. Our results are consistent with MnSOD being a tumor suppressor gene in human prostate cancer.
Oncogene (2005) **24,** 77–89. doi:10.1038/sj.onc.1208145
Published online 15 November 2004

Keywords: superoxide dismutase; prostate cancer; reactive oxygen species; cell cycle; overexpression; hydrogen peroxide

Introduction

Reactive oxygen species (ROS) are generated as a byproduct of cellular aerobic metabolism; production of ROS is amplified when cells are exposed to various stress conditions (Bae *et al*., 1997; Suzukawa *et al*., 2000). In mitochondria, ROS are generated as a result of normal biochemical reactions using oxygen (Chance *et al*., 1979). ROS includes superoxide, hydroxyl, and peroxyl radicals as well as hydrogen peroxide (H_2O_2) and like molecules. High levels of ROS can be detrimental to cells. Mitochondria are considered as the most important cellular source of ROS and may be susceptible to oxidative damage. ROS can modify cellular protein, lipid, and DNA, which results in altered functions of the cell (Klaunig *et al*., 1998). It has been reported that ROS, when present at high levels, may play a key role in the mechanisms of initiation and progression of disease such as carcinogenesis (Oberley and Buettner, 1979; Cerutti, 1985; Church *et al*., 1993; Zhong *et al*., 1996), and disease associated with aging (Orr and Sohal, 1994). However, when present at normal levels, ROS have important physiologic functions, for example, regulation of signal transduction pathways (Chen *et al*., 1995b; Monteiro and Stern, 1996), mitosis (Murrell *et al*., 1990; Oberley *et al*., 1991), cell differentiation (Allen and Balin, 1989), and activation of gene transcription factors (Li *et al*., 1998a; Schreck *et al*., 1991). Over the last three decades, a great deal of evidence has been gathered linking ROS to cancer via oxidative events.

Oxidative changes occur in cellular components when the balance shifts between the rate of production of ROS and the rate of removal by antioxidants and antioxidant enzymes. Antioxidant enzymes prevent or terminate the reactions of ROS, thereby preventing these processes. The primary antioxidant enzymes are the superoxide dismutases (SODs), catalase (CAT), and the glutathione peroxidases (GPx). SOD catalyses the dismutation of superoxide into H_2O_2 and oxygen, while CAT and GPx remove H_2O_2. The two major SOD enzymes in eucaryotic cells are manganese superoxide dismutase (MnSOD) found in mitochondria and copper zinc superoxide dismutase (CuZnSOD) found primarily in the cytoplasm. There are reports that tumor cells have lower antioxidant enzyme activity than their normal cell counterparts (Oberley and Buettner, 1979; Oberley and Oberley, 1986). One of the SOD enzymes commonly decreased or deleted in tumor cells is MnSOD. Restoring MnSOD activity has been shown in numerous studies to reverse the malignant phenotype of tumor

*Correspondence: GR Buettner, Free Radical and Radiation Biology, EMRB 68, The University of Iowa, Iowa City, IA 52242-1101, USA; E-mail: garry-buettner@uiowa.edu
Received 21 January 2004; revised 26 August 2004; accepted 26 August 2004; published online 15 November 2004

cells. It has been reported that increasing the expression of MnSOD suppresses the malignant phenotype of human breast cancer cells, MCF-7 (Zhang *et al*., 1999); human glioma cells, U118-9 (Wang *et al*., 1997); human oral squamous carcinoma cells, SCC-25 (Liu *et al*., 1997); human pancreatic cancer cells, MIA PaCa-2 (Weydert *et al*., 2003); mouse fibrosarcoma, NIH/3T3 cells (Li *et al*., 1998b); and human melanoma cells, UACC-903 (Church *et al*., 1993). Thus, in a large number of different cancer cell types, MnSOD overexpression inhibits cancer cell growth. Thus, it is essential to study whether androgen-independent prostate cancer is also responsive to MnSOD overexpression.

Human prostate cancer is the most commonly diagnosed malignancy among men and the second leading cause of cancer death in the US, most dying from metastatic disease (Foster *et al*., 1999). The major difficulty is the lack of effective mechanism-based treatment for the disease. Tumor resistance to conventional therapies, such as chemotherapy or radiation, presents a major problem in cancer treatment today; one such example is prostate cancer at its later stage. Failure to eradicate advanced resistant tumors with conventional therapies has led to the investigation of novel therapeutic approaches like gene therapy. Gene therapy approaches are being considered that target the expression of genes that lead to the removal of ROS at important cellular sites. The use of MnSOD, which removes superoxide arising from various oxidative stresses, is one such possible therapy.

MnSOD is a crucial antioxidant enzyme protecting mitochondria against oxidative stress (Sun, 1990; Liochev and Fridovich, 1997). The importance of MnSOD is evidenced by the multiplicity of reports indicating that MnSOD is a tumor suppressor gene in many cell types. In view of this evidence, we were interested in studying the role of MnSOD in the androgen-independent prostate cancer cell line (PC-3). Although it has been studied in other cell lines, the rationale for investigating the validity of the hypothesis that MnSOD could be a tumor suppressor gene in the PC-3 cell line is multifold. In contrast to the usual tumor suppressive effect of MnSOD, MnSOD overexpression has also been shown to increase the growth of one cancer cell line: cervical carcinoma cells (Palazzotti *et al*., 1999). Therefore, the tumor suppressive effect could be cell type specific. The mechanism by which MnSOD affects cancer cells varies among cancer cell types and their antioxidant capacity. Also, prostate cancer cells are either androgen dependent or androgen independent. It is known than MnSOD slows the growth of DU145, an androgen-independent cell line (Li *et al*., 1998c). Jung *et al*. (1997) have shown that different prostate cancers have varying levels of antioxidant enzymes and therefore could have different responses to treatment. Since, PC-3 cells are androgen independent, MnSOD may influence these cells differently. Androgen-independent prostate cancer cells are more resistant to many known cancer therapies than androgen-dependent tumors. Therefore, we wanted to determine whether or not MnSOD has a tumor suppressive effect in PC-3, an androgen-independent human prostate cell line.

This work demonstrates for the first time that MnSOD overexpression causes growth inhibition both *in vivo* and *in vitro* in PC-3 cells. Moreover, MnSOD-overexpressing cells demonstrated: (1) G_1 cell cycle delay, (2) increased mitochondrial membrane potential, and (3) increased flux of H_2O_2. These results suggest new treatments strategies for androgen-independent prostate cancer.

Results

Stable transfection of MnSOD

Comparison of MnSOD levels in prostate cancer cells (PC-3) to nonmalignant prostate cells It is known that the antioxidant defense-related enzymes are generally modified in tumor cells, which might be related to their growth. In order to verify whether the level of MnSOD is different in PC-3 cells compared to nonmalignant immortalized human prostate epithelial cells (P69SV40T), MnSOD protein and activity were measured. Even though these nonmalignant cells are not completely normal due to their immortalization, P69SV40T cells were considered as a good representation of normal prostate epithelial cells. The characterization of P69SV40T cell line was carried out by Bae *et al*. (1994, 1998). The MnSOD protein was measured with Western blot and the protein band corresponding to the MnSOD in PC-3 Wt cells was $\sim 50\%$ of that of nonmalignant immortalized human prostate cells (P69SV40T) (Figure 1a). Similar results were found with MnSOD activity when comparing Wt cells with P69SV40T cells (Figure 1b).

PC-3 clonal cell lines overexpressing MnSOD Three stably transfected clonal cell lines along with a vector control were isolated in order to determine the effect of differences in levels of MnSOD on cell growth characteristics. MnSOD protein and activity in these transfectants were measured in cell lysates. As determined with Western blotting, there was an increase in MnSOD immunoreactive protein in the clones transfected with MnSOD cDNA (Figure 2a). As expected, the MnSOD activities were also significantly increased and were sevenfold greater than the basal parental Wt cells ($P<0.0001$) (Figure 2b and c). The increases in MnSOD activity of the three overexpressors Mn5, Mn32, and Mn98 were 7.4-, 8.3-, and 8.2-fold, respectively, and that of Neo was 0.7 of parental cells. Although the MnSOD activities were not very different from each other among the overexpressors, we wanted to examine how different clones with nearly equal levels of MnSOD behaved under the same circumstances. To determine the effect of increased MnSOD on the other antioxidant enzymes, CuZnSOD, CAT, and GPx activities were also measured (Table 1). CuZnSOD activity was below the limit of detection in the overexpressing clones in the enzymatic assay, but from

the activity gel the CuZnSOD activity can be determined and it was decreased to a similar small extent in the three overexpressing clones (data not shown) compared to Wt cells. However, one of the clones (Mn98) had less GPx and more CAT activity. Interestingly, the changes in both GPx and CAT were approximately a factor of three compared to the other two clones. The other two clones (Mn5, Mn32) had similar GPx and CAT activities. Therefore, two clones have almost the same levels of the measured antioxidant enzymes, while one clone has the same MnSOD level but different GPx and CAT levels.

In accordance with Western blot results for MnSOD overexpressors, there was also an increase in steady-state MnSOD mRNA levels. This was shown by Northern blot analysis for MnSOD mRNA (Figure 3a). A new MnSOD band was found; between 1 and 4 kb in size, in the overexpressing clones demonstrating that the increased MnSOD protein came from the transfected plasmid. A corresponding band in the Wt and Neo cells was not seen. The plasmid also increased the MnSOD mRNA level corresponding to both the 1- and 4-kb bands. Both 1- and 4-kb species could be detected and both were elevated upon transfection with MnSOD in

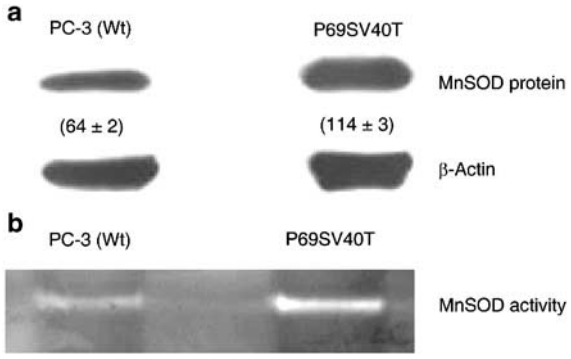

Figure 1 MnSOD protein and activity levels were decreased in PC-3 (Wt) cells compared to the nonmalignant immortalized prostate epithelial cells (P69SV40T). (**a**) Western blot analysis of protein: total protein from P69SV40T and PC-3 Wt cells were isolated, and 20-μg aliquots were loaded as described in the Materials and methods section. Immunoblotting was performed using an MnSOD polyclonal antibody (MnSOD, rabbit polyclonal IgG). Immunodetection was carried out using a goat anti-rabbit secondary antibody (1 : 10 000 dilution) and the enhanced chemiluminescence kit (ECL). The bands were visualized and quantified with a computerized digital imaging system using AlphaImager 2000 software (Alpha Innotech, San Leandro, CA, USA) and the densitometric numbers ($n=3$ measurements of one blot) $\pm$s.e. are given under each band normalized to β-actin. (**b**) Activity gel for MnSOD activity: a total of 200 μg of protein from each tumor of different cell clones were separated on an 8% native polyacrylamide gel with a 5% stacking gel. After electrophoresis, the gel was stained for MnSOD activity as described in the Materials and methods section. The achromatic band corresponding to MnSOD activity appeared on a blue background

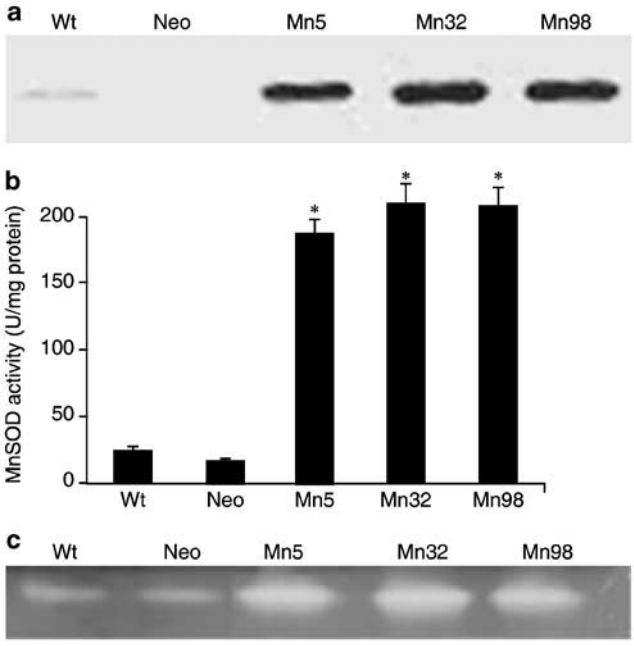

Figure 2 Transfection of PC-3 cells with MnSOD cDNA increased MnSOD protein and activity. (**a**) Western blot analysis of protein lysates from PC-3 cell lines to evaluate the expression of MnSOD protein: equal amounts of protein (25 μg) extracted from parental (Wt), PC-3/Neo, and three PC-3/MnSOD overexpressing clones (Mn5, Mn32, and Mn98) were electrophoresed and then transferred onto a nitrocellulose membrane. The blot was probed with a rabbit antiserum against human kidney MnSOD and the gels were stained with Coomassie blue and found to be equally loaded with protein. Immunoreactive protein was visualized using a chemiluminescent detection system. (**b**) MnSOD activity as measured by a spectrophotometric assay: the activity was assessed following the decrease in the rate of reduction of NBT at 560 nm upon addition of cell lysate in the presence of xanthine and xanthine oxidase. MnSOD activity was distinguished from CuZnSOD activity by its resistance to 5 mM sodium cyanide. The results are expressed as units per mg of total cellular protein. Values are means$\pm$s.e., $n=3$, for each cell clone. By one-way ANOVA, there is a significant difference in the mean values among the groups ($P<0.05$). *$P<0.0001$ *versus* Wt using Tukey's multiple comparison procedure. (**c**) MnSOD activity as determined by native gel electrophoresis: 100 μg of protein from each cell clone was separated on a 12% polyacrylamide gel. After electrophoresis, the gel was stained for MnSOD activity as described in the Materials and methods section

Table 1 Antioxidant enzyme activity in PC-3 cell lines[a]

Cell line	*MnSOD (U/mg protein)*	*CuZnSOD (U/mg protein)*	*GPx (mU/mg protein)*	*Catalase (mk/mg protein)*
PC-3 Wt	25$\pm$3.5	15$\pm$2.3	17.5$\pm$4.2	7.2$\pm$0.98
Neo	15.5$\pm$2.7	71$\pm$7.5	19$\pm$3.5	6.8$\pm$1.0
Mn5	185$\pm$2.3*	ND[b]	8.8$\pm$0.4	7.0$\pm$0.46
Mn32	208$\pm$1.7*	ND[b]	8.5$\pm$4.8**	10.1$\pm$1.5
Mn98	205$\pm$1.2*	ND[b]	3.0$\pm$1.0	26.7$\pm$0.86

[a]Values are mean$\pm$s.e.m. of three independent cultures. [b]not detectable. *$P<0.001$ *versus* PC-3 Wt cells. **$P<0.05$ *versus* PC-3 Wt cells

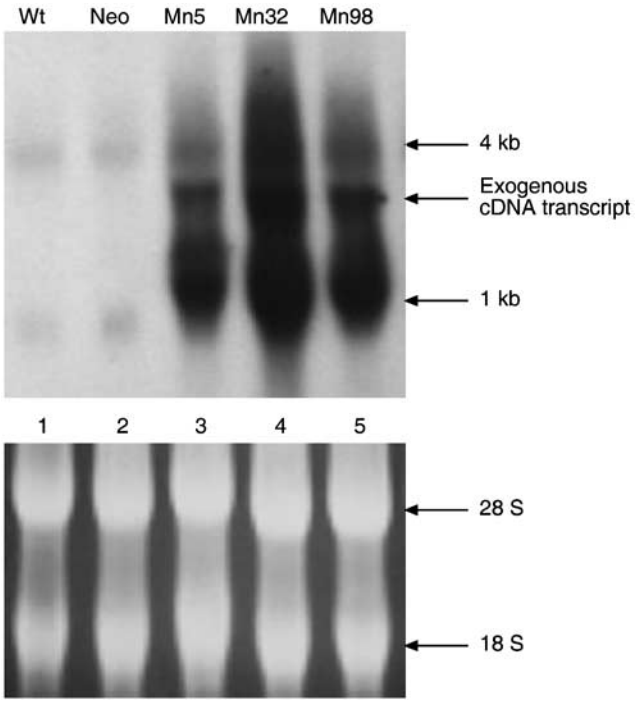

Figure 3 Transfected MnSOD cDNA was expressed in PC-3 cells as determined by Northern blot analysis. Equal amounts of RNA extracted from parental (Wt) PC-3 cells, PC-3/Neo, and PC-3/MnSOD overexpressors were electrophoresed and transferred to a UV-crosslinked nylon membrane. The Northern blot was probed with digoxigenin-dUTP-labeled MnSOD cDNA. The blots were exposed to Kodak XAR film at room temperature. (**a**) The autoradiograph of the hybridized blot shows the mRNA transcript of human MnSOD present, between 1 and 4 kb, in the MnSOD overexpressors. (**b**) UV254 nm-visualization of 18S and 28S bands for both the gels and membranes show the equal loading of the samples. The lanes 1–5 represent cell lines Wt, Neo, Mn5, Mn32, and Mn98 respectively

the three clones. The parental (Wt) PC-3 cells and vector control (Neo) cells had very low MnSOD mRNA levels. Equal loading of the samples was verified by UV254 nm visualization of 18S and 28S bands for both the gels and membranes as shown in Figure 3b. These results show that the transfected clones have increased levels of MnSOD gene expression.

Effect of MnSOD overexpression on the malignant phenotype

To unravel the role of MnSOD overexpression on the malignant phenotype of PC-3 cells, growth rate, cell doubling time (DT), anchorage-independent growth, and tumorigenicity in nude mice were determined.

Effect of MnSOD transfection on the growth of the PC-3 cell lines PC-3 clones that overexpressed MnSOD activity had a slower growth rate *in vitro* than the Wt cells, Figure 4a. Each of the three MnSOD overexpressors have different growth rates; all grew slower than the parental Wt cells. The reason why the Neo cells grew slower than the Mn5 cells is not clear. Clones Mn32 and Mn98 had the slowest growth rate. On day 9

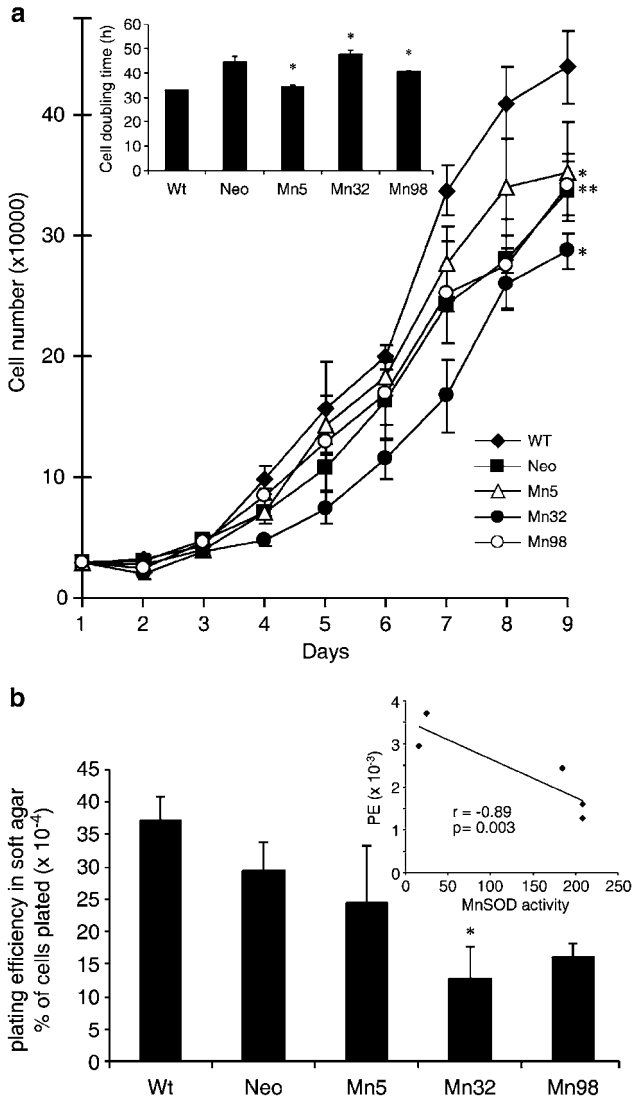

Figure 4 MnSOD overexpression inhibited PC-3 cell growth in culture. Cells (3×10^4) were seeded into 24-well plates. (**a**) Growth curve: the cell number in three to five flasks was determined at different time intervals. MnSOD-overexpressing clones had a slower growth rate than the parental cells (Wt). The slowest growth rate was observed in the Mn32 clone, which had the highest overexpression of MnSOD. On day 9, cell growth was decreased about 50% in the Mn32 cells when compared to parental cells. Statistical analysis by two-way ANOVA shows that there is a significant difference among groups and days ($P<0.0001$). Pairwise statistical comparison on day 9 were $*P<0.0001$; Mn5 *versus* Wt, Mn32 *versus* Wt, and $**P=0.0002$ for Mn98 *versus* Wt. The inset shows the cell DT: from the cell growth curve, DT was calculated and plotted as mean$\pm$s.e. The Mn32 cell clone had the slowest growth rate with a DT of 47 h. By Dunnett's multiple comparison, Wt is significantly different from Mn5, Mn32, and Mn98 ($*P<0.0001$). (**b**) Plating efficiency in soft agar. Experiments were performed as described in the Materials and methods section. The colony formation was quantitated by counting colonies containing >50 cells. The experiment was repeated eight times with cells from eight different cultures. Values are means$\pm$s.e. By one-way ANOVA, there is a significant difference in the mean values among the groups ($P<0.05$) and $*P=0.028$ for Mn32 *versus* Wt using Tukey's multiple comparison procedure. The inset depicts the correlation analysis of colony formation in soft agar *versus* MnSOD activity ($r=-0.89$, $P=0.003$)

after plating, the Mn32 clone had an approximately 50% slower growth rate than the parental Wt cells. In summary, there was a significant inhibition in the growth *in vitro* of MnSOD-overexpressing cells compared to the parental Wt PC-3 cells ($P<0.05$).

The DTs of MnSOD-transfected clones Mn5, Mn32, and Mn98 were 34, 47, and 44 h, respectively, which compared to 33 h for Wt cells (inset). The DT of Mn5 was unexpectedly lower than the other clones. To understand this apparent anomaly, the influence of other antioxidant enzymes was checked (Table 1). However, correlation analysis of GPx or CAT or combinations to MnSOD activity in Mn5 cells did not explain the discrepancy in growth rate.

Effect of MnSOD overexpression on the growth of PC-3 cells in soft agar To further investigate the effect of MnSOD on PC-3 cell growth inhibition, anchorage-independent growth in soft agar was examined. Malignant cells in general have higher ability to form colonies in soft agar than nonmalignant cells. For this experiment, a single cell suspension was seeded in 0.5% agar and allowed to form colonies. The results are shown in Figure 4b. The MnSOD-overexpressing PC-3 cell line had significantly lower plating efficiencies in soft agar compared to that of parental Wt cells with Mn32 being statistically different ($P=0.028$). Regression analysis of plating efficiency with MnSOD activity showed an inverse linear correlation ($r=-0.89$, $P=0.003$).

Effect of MnSOD overexpression on tumor growth in nude mice PC-3 cells (Wt, Neo, or MnSOD overexpressors) were injected subcutaneously into nude mice and tumor growth was followed. Palpable tumors were formed 12–14 days after the injection. All three MnSOD-overexpressing cell lines formed tumors that grew much more slowly than the parental Wt and Neo cells, Figure 5a. Parental and Neo cell lines formed larger tumors than the MnSOD overexpressors. The growth of

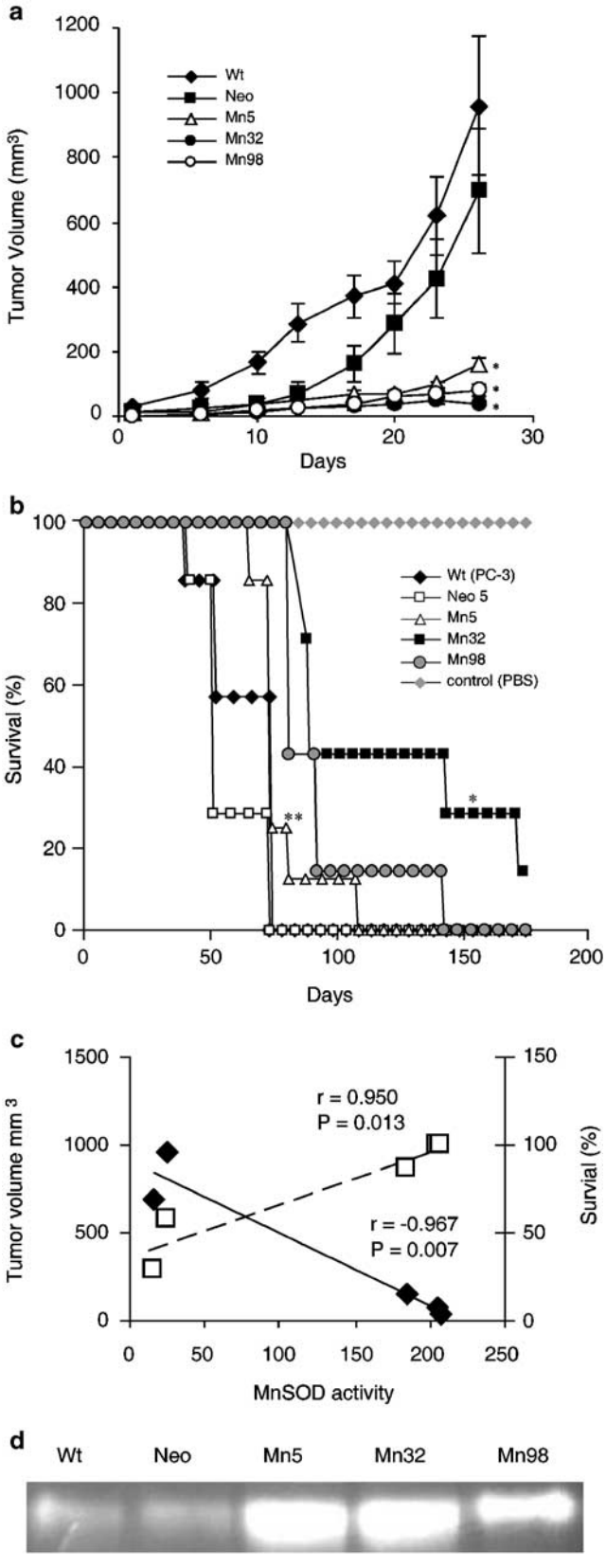

Figure 5 Overexpression of MnSOD decreased the tumorigenicity of PC-3 cells in nude mice. (**a**) Tumor volume: cells (1×10^6) in PBS were subcutaneously injected in the flank region of nude mice. Tumor length (L) and width (W) were measured twice a week after tumors were visible. Day one is 13 days after the injection of cells. Tumor volume was calculated by $(L\times W^2)/2$. The results represent mean ± s.e. ($n=8$). *$P<0.0025$ compared to the PC-3 Wt cells on day 26 using Bonferroni's multiple comparison procedure (day 26: median tumor volume of Wt was 960 mm^3; Neo was 660 mm^3) (**b**) Effects of MnSOD on the survival of mice bearing PC-3 xenografts: Mice were killed when they were moribund. The survival curve of mice injected with Mn32 cells was significantly longer than that of control. The tumors were removed for further analysis. According to the log-rank test, a statistical significance of *$P=0.0004$ comparing Mn32 *versus* Wt, Mn5 *versus* Wt, and **$P=0.043$ for Mn98 *versus* Wt. (**c**) Correlation analysis of tumor volume *versus* MnSOD activity, on day 26 after the tumors became visible (♦; $r=-0.967$, $P=0.007$) and percentage survival of mice *versus* MnSOD activity on day 82 (□; $r=0.950$, $P=0.013$). (**d**) Activity gel analysis of tumor tissues removed from mice: tumors were homogenized and protein analyses were performed. Equal amounts of protein were loaded on 12% polyacrylamide gel, electrophoresed, and stained for MnSOD. The tumors removed from mice inoculated with Mn98 cells had reduced MnSOD activity *in vivo* compared to *in vitro* level, but the activity was still increased compared to the controls. All other tumors retained the MnSOD activity as *in vitro*

MnSOD overexpressors of PC-3 cell lines were reduced by 75% compared to the parental Wt cells. All three MnSOD-overexpressing clones had significantly decreased growth rates compared to the parental and Neo cells ($n=8$, $P<0.05$). The tumor incidence was found to be same for all cell lines (data not shown). There was also a significant difference among the groups (Wt, Neo, and three MnSOD overexpressors) in mean tumor volume ($P=0.0023$) by linear mixed model analysis.

The tumors were allowed to grow to a volume of about 1000 mm^3 (this was considered as the time of killing) at which time the mice was euthanized and the tumors were removed. The mice bearing tumors of Wt cells reached the time of killing on day 26 after the injection of tumor cells into mice. The tumor sizes in all mice were measured until they were euthanized. From the survival data as shown in Figure 5b, it is clear that MnSOD-overexpressing clones had longer survival than the parental and plasmid control cell lines. Thus, MnSOD overexpression decreased the growth of tumor xenografts in mice and at the same time increased the median survival of prostate cancer-bearing mice. The mice that were inoculated with Mn98 cells had shorter survival times than those inoculated with Mn32 cells, even though the MnSOD activity is the same in both. At a specified time, tumor volume was inversely proportional to MnSOD activity and the survival of mice was directly proportional to the MnSOD activity with significant correlation (Figure 5c).

At 5–6 weeks after inoculation of the mice, tumors were surgically removed, weighed, and the tissue was homogenized. In one out of eight mice that were inoculated with the Mn32 clone, the tumor grew to a volume of 80 mm^3 before shrinking and then eventually disappearing. Interestingly, four out of seven tumors grown from Mn5 cells were covered with blood vessels, which was not seen in tumor tissues from other cell lines.

The MnSOD activity was measured in the tumors removed from the euthanized mice from all PC-3 cell lines using activity gels, Figure 5d. A high level of MnSOD activity was retained in the Mn5 and Mn32 clones *in vivo*, but the MnSOD activity was found to be somewhat reduced in the Mn98 clone. Still all three clones had higher MnSOD activity *in vivo* compared to Wt. The tumor incidence of all cell lines was the same in nude mice. Thus, in the PC-3 cell line, increased expression of MnSOD greatly suppressed tumor volume, but had no effect on tumor incidence. The effect of tumor suppression by the antioxidant enzyme MnSOD *in vivo* was found to be much greater than the growth inhibition *in vitro*. It is likely that factors like oxygen availability and other host factors could be the cause of the difference between *in vivo* and *in vitro* results. Also, no metastases were visible from the inoculation of any of the PC-3 cells into nude mice. These results clearly demonstrate that the mitochondrial antioxidant enzyme, MnSOD, is capable of partially suppressing the growth *in vivo* of malignant PC-3 cells.

Effect of MnSOD overexpression on the production of H_2O_2 Superoxide when produced in mitochondria, if left unchecked, could damage mitochondria. MnSOD protects mitochondria by converting superoxide into H_2O_2. MnSOD overexpression has been shown by indirect methods to lead to an increase in the levels of H_2O_2 (Panus *et al*., 1993). Thus, we were interested in measuring the level of H_2O_2 in PC-3 cells. H_2O_2 produced intracellularly can diffuse out of the cell (Antunes and Cadenas, 2000) and thus can be measured in the media. The higher the steady-state level of H_2O_2 in the cell, the greater will be the accumulation of H_2O_2 in the media. To determine whether PC-3 cells overexpressing MnSOD have higher levels of H_2O_2, we measured extracellular H_2O_2 directly using an organic indicator (pHPA, *para*-hydroxy phenyl acetic acid) in the presence of horseradish peroxidase (HRP).

The ratio of changes in H_2O_2 levels in all PC-3 cell lines compared to basal levels in Wt cells are given in Figure 6a. As seen clearly from Figure 6a, the MnSOD overexpressors Mn32 and Mn98 had increased levels of H_2O_2 as detected directly in the media compared with the parental Wt cell line. There was a significant increase in the production of H_2O_2 by Mn32 cells, 53% more than Wt cells ($P=0.01$). The increase in H_2O_2 in Mn32 clone was $\sim$1.9-fold and in Mn98 was $\sim$1.5-fold compared to Wt cells. The clone Mn5 had almost the same level of H_2O_2 as that of Wt cells. In addition, when compared to the empty vector, Neo, there was even a greater significant increase in H_2O_2 levels in MnSOD overexpressors; Mn5 ($\sim$1.7-), Mn32 ($\sim$3.3-), and Mn98 ($\sim$2.6-) fold when compared to Neo.

Effect of MnSOD overexpression on the mitochondrial potential of PC-3 cells Mitochondrial membrane potential is the result of asymmetric distribution of charges between the inner and outer sides of the inner mitochondrial membrane. This gradient drives the synthesis of ATP. Thus, mitochondrial membrane potential could reveal mitochondrial functionality and the energy status of a cell. The main source of ROS in most cells is from the mitochondria. One parameter that is altered due to the production of ROS is mitochondrial transmembrane potential. Therefore, the effect of varying the levels of MnSOD on membrane potential was determined using the fluorescent dye Rhodamine 123 (Rh 123). Rh 123 is taken up preferentially by mitochondria. Changes in transmembrane potential are reflected by the change in the mitochondrial concentration of the dye. The greater the integrity/function of the membrane, the more dye that will be taken up and therefore a higher intensity of fluorescence will result. If the membrane is damaged and leaky, then the fluorescence intensity corresponding to Rh 123 dye uptake decreases. Thus, the amount of fluorescence from the dye Rh 123 correlates directly to mitochondrial membrane potential.

To check the consistency of the results, another fluorescent dye JC-1 (5,5′, 6,6′-tetrachloro-1,1′,3,3′-tetraethylbenzimidazolcarbocyanine iodide) was used to measure the membrane potential. JC-1 is a cationic lipophillic dye and exhibits potential-dependent

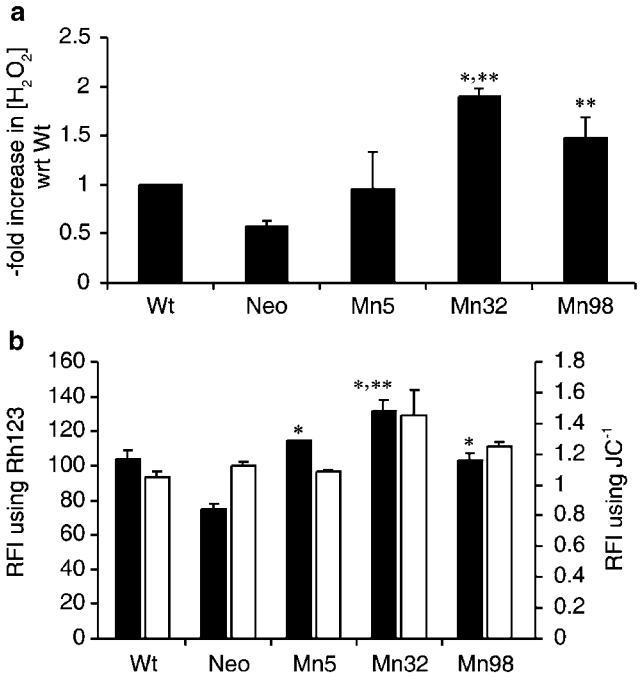

Figure 6 Phenotype of transfected cells. (**a**) MnSOD overexpression increased the extracellular production of H_2O_2: release of H_2O_2 by PC-3 cell lines in the presence of pHPA/HRP was measured spectroflurometrically (as described in Materials and methods). The amount of pHPA dimer formed is directly proportional to the amounts of H_2O_2 formed over a period of 1 h. The concentration of H_2O_2 released per cell was standardized with the known concentrations of H_2O_2. Using one-way ANOVA, there is overall significant difference among groups ($P<0.05$) and using Tukey's multiple comparisons, there was a significant difference between Mn32 *versus* Wt $*P=0.01$, Neo *versus* Mn32, and Neo *versus* Mn98, $**P<0.05$. (**b**) MnSOD increased mitochondrial membrane potential: aliquots of 5×10^6 cells were incubated in PBS containing 25 μM Rh 123 for 30 min at room temperature or 1 μg/ml of JC-1 for 10 min at 37°C in the dark. Samples were then pelleted, resuspended in PBS, and immediately analysed. For the simultaneous evaluation of cell viability, cells were stained with PI and analysed with flow cytometry. Solid bar (■) shows the relative fluorescent intensity (RFI) using Rh 123 and the open bar (□) shows the ratio of RFI between 585 and 530 nm using JC-1. According to one-way ANOVA, there is a significant difference among the groups in the mean Rh 123 ($P<0.0001$). By Tukey's *post hoc* procedure, the following pair-wise comparison were significant; $*P<0.05$ for Neo *versus* Mn5, Mn32, Mn98, and $**P<0.05$ for Wt *versus* Mn32. Values are mean ± s.e. of $n=3$

accumulation in mitochondria. When the membrane integrity increases, there will be a fluorescence emission shift from green (530 nm) to red (585 nm). In the presence of higher membrane potential, JC-1 forms J-aggregates, which increases fluorescence intensity at 585 nm (Reers *et al*., 1991), and therefore the fluorescence intensity ratio of 585–530 nm increases. We compared the membrane potential of parental PC-3 Wt and Neo vector control cell lines to the MnSOD overexpressors.

The relative fluorescence intensity corresponding to the membrane potential of cells exposed to either Rh 123 or JC-1 is given in Figure 6b. The transfection of PC-3 cells with MnSOD showed an increase in the membrane potential using Rh 123. The fluorescent intensity of Rh 123 in MnSOD-overexpressing clones was higher than parental Wt and Neo cells. The cellular retention of the dye Rh 123 by the MnSOD clone (Mn32) was increased by 76% over that of Neo cells ($P<0.05$). The membrane potential of the other two clones Mn5 and Mn98 were also higher ~1.5 times more than that of Neo cells using the dye Rh 123 ($P<0.05$). Also, the fluorescence intensity corresponding to the J-aggregate formation increased in Mn32 cells (~1.4-fold) compared to Wt and Neo cells. These observations imply that higher steady-state levels of superoxide in the mitochondria decrease the mitochondrial membrane potential, probably by disruption of the membrane.

Effect of MnSOD overexpression on the PC-3 cell cycle progression To determine whether growth inhibition in the MnSOD-overexpressing PC-3 cells is due to a cell cycle phase redistribution effect, flow cytometric analyses of bromodeoxyuridine (BrdUrd) pulse-labeled parental Wt, Neo, and the overexpressors (Mn5, Mn32, Mn98) were performed, Figure 7. It is clear that there was a change in the distribution of cells in G_1, S, and G_2 phases of the cell cycle as a result of MnSOD transfection; in the Mn32 clone, 64% of the MnSOD-transfected cells were in G_1 phase, while only 48.5% of the parental Wt and 44% of the Neo cells were in G_1 (statistically different at $P<0.05$). The S phase distribution between the Neo and Mn32 clones was 39.9% *versus* 28.5% ($P=0.002$). There is also a statistically significant ($P<0.05$) decrease in G_2+M fraction in the Mn32 clone (7.5%) compared to Wt (~13%) and Neo cells (~16%). The changes in the other MnSOD-overexpressing clones were significant; 51% in Mn5 and 52% in Mn98, clones were in G_1 phase and ~13–14% in G_2+M phase, which is statistically different ($P<0.05$) compared to Neo cells. A considerable increase in G_1 fraction in Mn32 cells and a moderate increase in Mn5 and Mn32 cells suggest that the MnSOD-induced delay in cell growth could be associated with a slower progression from G_1 to S.

Discussion

First, to test the hypothesis that the antioxidant enzyme MnSOD is altered in tumor cells compared to their nonmalignant cell counterpart, MnSOD activity and protein were determined. MnSOD protein was lower (~twofold; by densitometric analysis) in the parental PC-3 cells compared to the immortalized nonmalignant human prostate epithelial cells (P69SV40T) (Figure 1a). Correspondingly, the MnSOD activity also was found decreased in parental Wt cells compared to P69SV40T cells (Figure 1b). Therefore, under these growth conditions, there was a decrease in the level of MnSOD in androgen-independent PC-3 cells compared to its normal cell counterpart. However, since the cells were grown in different media and different oxygen concentrations, further work is necessary to confirm this observation.

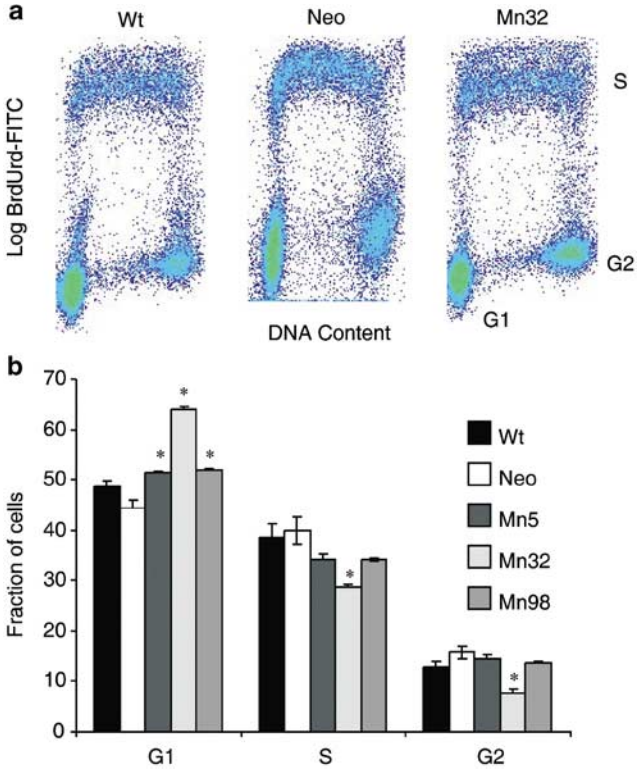

Figure 7 Cell cycle delay by overexpression of MnSOD in PC-3 cells. Exponentially growing asynchronous parental Wt cells, vector control Neo, and one of the MnSOD overexpressors, Mn32, were pulse-labeled with BrdUrd, trypsinized and fixed with 70% ethanol. Nuclei were isolated and immunostained using antibodies to BrdUrd and fluorescein isothiocyanate (FITC)-conjugated mouse goat anti-mouse IgG. Nuclei were counterstained with PI containing RNase A and analysed for the DNA content by flow cytometer. Top panel: Representative contour plots of dual parameter PI *versus* log. BrdUrd-FITC histograms of PC-3 Wt, Neo, and Mn32 cells. Positions of cells in G_1, S and G_2 are labeled in the right panel histogram. Bottom Panel: Distribution of cells in G_1, S, and G_2+M phases were calculated using Cell Quest software. According to one-way ANOVA, there is a significant difference among the groups in the mean G_1, S, and G_2+M phases ($P<0.05$) of the cell cycle. By Tukey's *post hoc* comparison, a significant difference in the mean of G_1 and G_2+M values was found to be $^*P=0.0011$ and $^{**}P=0.0001$, respectively, for Mn32 *versus* Wt. Values are mean $\pm$ s.e. of three independent cultures

The antioxidant enzyme MnSOD is known as a tumor suppressor in many cancer cell types. To test whether or not MnSOD is indeed a tumor suppressor gene in androgen-independent prostate cancer cells, both *in vitro* and *in vivo* studies were carried out with PC-3 cells to measure any growth inhibitory effects of MnSOD on this cell line. We stably transfected PC-3 cells with MnSOD cDNA and isolated three MnSOD overexpressors (Mn5, Mn32, Mn98). Parental, plasmid-transfected control, and these three MnSOD-overexpressing clones were studied. The mRNA, protein, and activity of MnSOD were increased in all three overexpressing clones. MnSOD overexpression significantly reduced the growth rate and inhibited anchorage-independent growth of PC-3 tumor cells. Prolonged animal survival probably due to reduced tumorigenicity was found in mice inoculated with each of the overexpressors. These studies show that MnSOD inhibits the growth of androgen-independent prostate cancer cells *in vitro* and *in vivo*.

The growth inhibition of tumors by MnSOD overexpression *in vivo* was more pronounced than observed with the *in vitro* study. The two clones Mn32 and Mn98 had almost the same levels of MnSOD activity, as measured by inhibition assay, yet they had different growth rates. Changes in the levels of MnSOD can alter the levels of other antioxidant enzymes. Therefore, to narrow down the role of MnSOD, the influence of other antioxidant enzymes was also considered. Levels of CuZnSOD might affect the malignant phenotype. For example, CuZnSOD overexpression in U118-9 cell line was found to inhibit the growth of brain cancer cells (Zhang *et al*., 2002b). In the present study, the CuZnSOD activity level decreased to a similar extent in all the MnSOD overexpressors compared to the parental Wt cells. However, the absolute value of the loss of activity is small compared to the gain in MnSOD activity. Thus, the influence of CuZnSOD on the growth rate could be considered minimal.

Comparing the levels of CuZnSOD between Wt and Neo, the CuZnSOD activity was increased significantly in Neo ($P<0.05$), compared to Wt cells. This increased level of CuZnSOD could be the reason for the increased DT in the *in vitro* studies. However, more importantly in the *in vivo* studies, both Wt and Neo showed similar behavior. The inhibition of growth of tumor cells overexpressing MnSOD in nude mice, which is a definitive study to test malignancy, clearly depicts MnSOD as a tumor suppressor gene.

Considering the other antioxidant enzymes, the Mn98 clone had three times more CAT but only one-third the activity of GPx compared with Mn32 clonal cells. This could be the reason for the different growth rate between the clones. The changes in antioxidant enzymes could be due to clonal selection or adaptation.

Several factors could alter the growth of tumor cells *in vivo*. Therefore, tumor tissue from the mice was examined. From external observations of the tumor tissue, it could be seen distinctly that four out of seven mice that had tumors from Mn5 clones were covered with blood vessels. Mice that received the Mn5 cells had more rapid growth of tumors and shorter survival times compared to the other two overexpressing clones. However, all three overexpressors had much slower growth rate than the Wt and Neo cell lines *in vivo*. The reasons for differences *in vitro* and *in vivo* studies could be because increased vascularization may have contributed to the faster tumor growth of Mn5 *in vivo* (Chin *et al*., 2003).

If the MnSOD activity of the tumors that developed from cells overexpressing MnSOD were to change *in vivo*, then a change in the growth rate of the tumor might result. The MnSOD activity was retained in all tumor tissues except those from the Mn98 cells. The MnSOD activity of the tumor tissues taken from the nude mice that received Mn98 cells was decreased

compared to its *in vitro* activity, but still its MnSOD activity was higher than that of the tumors from the parental Wt cells. It is not known when the activity could have gone down *in vivo*. However, we speculate that the MnSOD activity may have gone down towards the end of the *in vivo* experiment because the growth rate of the tumor remained slower until then.

A noticeable increase in MnSOD mRNA expression was found in the Mn32 clone compared to the other two MnSOD-overexpressing clones. *In vitro*, the Mn32 clone had the slowest growth rate and reduced anchorage-independent growth compared to other two clones. The greatest reduction in tumor growth was seen in the Mn32 clone compared to tumors in mice bearing the Mn5 and Mn98 clones. This corresponds with the longer survival time of mice bearing Mn32 cells. Therefore, the higher the MnSOD level, the greater was the growth inhibitory rate in PC-3 cells. Interestingly, one of the seven mice that received Mn32 cells grew a tumor to a size of 4 mm × 5 mm and then it receded slowly.

To understand the mechanism of action of MnSOD overexpression, several possibilities can be suggested. Oberley and co-workers have shown indirectly that H_2O_2 levels increase in cell lines as a result of MnSOD overexpression (Li *et al*., 1998a; Zhang *et al*., 2002a). In addition, Rodriguez *et al*. (2000) have indirectly, by CAT transfection, shown that the antiproliferative effect of MnSOD may be due to increased H_2O_2 production as a result of MnSOD overexpression, which also enhances net ATP production and respiratory chain activities. Li *et al*. (2000) showed similar reversal of tumor growth inhibitory effects of MnSOD overexpression with GPx transfection. In the present study, we measured extracellular levels of H_2O_2 directly; the overexpressing clone (Mn32) had increased levels of H_2O_2 compared to that of Wt and Neo cells. The clone, Mn98 having the same level of MnSOD activity as that of the Mn32 clone, showed a lower level of H_2O_2 compared to Mn32 clone. The possible reason for the decreased rate of release of H_2O_2 could be that the clone Mn98 has ~threefold increase in CAT compared to the other two MnSOD-overexpressing clones. The reason why the Mn5 has much lesser release of H_2O_2 compared to the other two clones with almost same levels of MnSOD activity is not clear. However, if H_2O_2 is one of the main player in the control of proliferation in cells overexpressing MnSOD, then these results could explain the differences in the growth rate among the three overexpressors having almost the same level of MnSOD activity. Therefore, the growth suppression could be due to inhibition of cell proliferation. Thus, one possibility for the inhibitory growth effect of overexpressing MnSOD in PC-3 cells could be due to increased H_2O_2 production (Li *et al*., 2000).

MnSOD can inhibit the growth rate of a cancer cell population by either altering the rate of cell proliferation or the rate of cell death. High levels of H_2O_2 can cause cell death. Examining the mode of cell death with Annexin V, and flow cytometric analysis, MnSOD overexpression did not cause an increase in cancer cell killing by necrosis, apoptosis, or senescence (checked by β-gal assay) (data not shown). Also, gel electrophoresis analysis for DNA fragmentation excluded the possibility of apoptosis as a cause of the decreased growth rate of overexpressors (data not shown). So MnSOD does not appear to cause increased prostate cell killing and could be affecting the cells by inhibiting cell proliferation, consistent with MnSOD contributing to the overall redox environment of the cell (Schafer and Buettner, 2001).

Several studies using human diploid fibroblasts showed that H_2O_2 induced a G_1 growth arrest (Chen *et al*., 1995a; Chen *et al*., 1998; Chen *et al*., 2000). Also, Barnouin *et al*. (2002) have shown multiphase cell cycle arrest in mouse fibroblasts induced by H_2O_2. Here, in our studies, the H_2O_2 produced by Mn32 cells was ~1.9-fold greater than the parental PC-3 cells. In the other two clones Mn5 and Mn98, the H_2O_2 released was somewhat less than in Mn32 cells. Therefore, to determine if MnSOD slows the cell proliferation in PC-3 cells, cell cycle study was undertaken; the differences in the growth rate among similar MnSOD clones may partially be due to cell cycle delay or arrest. MnSOD overexpression increased the fraction of cells in the G_0/G_1 phase and correspondingly decreased the fraction of cells in S and $G_2 + M$ phases compared to the Wt and Neo. The increase in G_0/G_1 fraction as a result of MnSOD transfection in Mn32 cells (64 *versus* 48.5%) suggests that the growth inhibition by MnSOD overexpression could be due to the slower progression from G_1 to S. The progression of Neo, the vector control, was even faster, as more cells moved to the S phase. In the other two clones, Mn5 and Mn98, the G_1 to S progression was still slower than Wt and Neo cells but faster than Mn32 cells. Thus, the inhibition of growth appears to be reflected in a delayed G_1 transit.

The intracellular level of H_2O_2 will alter the redox environment of the cell and thus influence progression through cell cycle, thereby changing the growth rate of MnSOD overexpressors differentially. A higher level of H_2O_2 will bring about a more oxidized cellular environment, which would result in slower growth (Schafer and Buettner, 2001). It is also known that H_2O_2 when produced in low amounts can act as vasodilator, thereby activating the mitochondrial K_{ATP} channels and results in the increase in its membrane potential (da Silva *et al*., 2003). This could contribute to the antiproliferative action of H_2O_2. Indeed we found that Mn32 cells had increased mitochondrial membrane potential compared to vector control cells (Neo) using two different fluorescent dyes. This is consistent with MnSOD lowering the steady-state levels of $O_2^{\bullet -}$ and thereby preventing oxidative membrane damage. Membranes with little or no oxidative damage should have higher membrane potential and a better function.

A general summary of the biochemical findings and the biological properties of the three MnSOD-overexpressing clones are presented in Table 2. It can be seen clearly that the levels of MnSOD and H_2O_2 correlate well with the parameters of cell growth and proliferation. Reduction in tumorigenicity *in vivo* and the partial reversal of the malignant phenotype *in vitro* is consistent with MnSOD being a tumor suppressor gene in these

Table 2 Overview of effects of MnSOD transfection

Property	*Mn5*	*Mn98*	*Mn32*
MnSOD activity (-fold wrt Wt)	7.4 (+)[a]	8.2 (++)	8.3 (+++)
mRNA	+	++	+++
H_2O_2 (-fold wrt Wt)	1	1.5	1.9
H_2O_2 (-fold wrt Neo)	1.7	2.5	3.3
Growth rate *in vitro*	+++	++	+
Growth rate in soft agar	+++	++	+
Doubling time	+	++	+++
Tumor growth	+++	++	+
MMP (RFI)			
Rh 123	+	++	+++
JC-1	+	++	+++
Cell cycle G_1%	51	52	64
S%	34	34	28.5
(G_2+M)%	14	13	7.5

[a] + < + + < + + +

androgen-independent prostate cancer cells. Our findings with these cells are consistent with many reports of decreased MnSOD expression in human cancers. Our results also indicate that MnSOD not only regulates cell survival but also affects cell proliferation by retarding the $G_1 -> S$ transition. Taken together, these data identify MnSOD as a tumor suppressor gene in prostate cancer and suggest it as a potential target for cancer therapy.

Materials and methods

Cell culture

The human prostate carcinoma cell line, PC-3, was purchased from the American Type Culture Collection (ATCC, Rockville, MD, USA). The PC-3 cells were cultured in modified Ham's F12 medium with 2 mM L-glutamine, 1.5 g/l sodium bicarbonate, 10% fetal bovine serum (FBS) (Hyclone), and 1% penicillin/streptomycin. The medium was changed every 4–5 days, and cells were routinely grown in 75-cm^2 vented tissue culture flasks at 37°C in a humidified atmosphere of 5% CO_2. Antibiotics were removed one passage before conducting experiments. For all experiments, cells were harvested when they were 70–80% confluent. The immortalized nonmalignant human prostate epithelial cell line, P69SV40T, was received from Dr Terry D Oberley's lab. These cells were grown in RPMI-1640 media, containing 5% FBS, at 4% O_2, 37°C and 95% humidity.

DNA transfection

PC-3 cells were stably transfected with the pcDNA3 plasmids, containing either a sense human MnSOD cDNA or containing no MnSOD insert. The transfection was performed with the indicated plasmid and the reagent LipofectAMINE (Life Technologies, Inc., Gaithersburg, MD, USA) according to the manufacturer's instructions. The clones were selected with 700 μg/ml of G418 (Geneticin; Life Technologies, Inc.) and isolated by cloning rings for further selection. The selected clones were grown in antibiotic-containing medium and screened by Western blotting for the level of MnSOD expression. Another cell line PC-3/Neo was established to serve as a vector control.

Protein analysis

The sample preparation for protein analysis was carried out on ice. Cells were washed three times with cold phosphate-buffered saline (PBS) and harvested by scraping followed by centrifugation at 200 *g* for 5 min at 4°C. The cell pellet was resuspended in potassium phosphate buffer (pH 7.8, 50 mM) and sonicated with three bursts of 20 s each using a Vibra Cell sonicator with a cup horn at full power (Sonics and Materials Inc., Danbury, CT, USA). The concentration of the protein was determined by the Bradford assay using bovine γ-globulin as a standard. Samples were then analysed for enzymatic activity.

Western blot analysis

Cells were washed thrice with PBS and harvested by scraping. The cell pellets were resuspended in 50 mM potassium phosphate buffer (pH 7.8) and sonicated. Protein levels were measured as described above. The samples were denatured with SDS loading buffer at 95°C for 5 min and then separated on a 12.5% SDS–PAGE. The protein was transferred to a nitrocellulose membrane (Schleicher and Schuell, Keene, NH, USA) and the gels were stained with Coomassie blue to check the protein loading. After blocking with 5% nonfat milk at room temperature for 2 h, the blot was incubated at 4°C overnight with rabbit antiserum against human kidney MnSOD made in our laboratory (30). Following this, the sample was incubated with an anti-rabbit IgG-horseradish peroxidase conjugate at room temperature for 1 h. The blots were developed using a chemiluminescence ECL Kit (Amersham, Arlington Heights, IL, USA).

Northern blot analysis

Total RNA was extracted using the RNAzol reagent according to the instructions from the manufacturer (Tel-test, Inc., Friendswood, TX, USA). The amount of RNA sample was quantified by spectrophotometry. RNA (30 μg) was loaded onto a 1.5% formaldehyde agarose gel and subjected to electrophoresis followed by transfer to a nylon membrane (Boehringer Mannheim, Indianapolis, IN, USA). The membrane was UV-crosslinked. Equal loading of the samples was verified by checking the 18S and 28S bands. A digoxigenin-dUTP labeled MnSOD cDNA probe was used to hybridize to the membrane under standard conditions. The blots were exposed to Kodak XAR film at room temperature.

Native gel assay

MnSOD activity was visualized by native PAGE according to the method described previously (Beauchamp and Fridovich, 1971). Cells were harvested and sonicated and the protein was quantified by the same method as described under Western blotting. Equal amounts of protein from different samples (usually 100 μg of cellular protein) were loaded onto a 12% polyacrylamide gel with a 5% stacking gel. Electrophoresis was performed in nondenaturing running buffer pH 8.3. After electrophoresis, staining of the gel was carried out by incubating in 2.43 mM NBT and 28 μM riboflavin/28 mM TEMED for 30 min in the dark. The gel was rinsed with distilled water and then illuminated under bright fluorescent light. The addition of 0.75 mM cyanide to the staining solution allowed for the detection of only the MnSOD activity by inactivating CuZnSOD. Achromatic bands corresponding to MnSOD appeared against a blue background.

Antioxidant enzyme activity (spectrophotometric) assays

The SOD activity was measured by the modified NBT method as described previously (Oberley and Spitz, 1985). Briefly, SOD activity was determined spectrophotometrically at 560 nm by measuring the reduction of NBT. The superoxide generated from the xanthine and xanthine oxidase system reduces NBT. However, in the presence of SOD, which converts superoxide to H_2O_2, the reduction of NBT is competitively inhibited. The amount of protein that inhibits NBT reduction to 50% of maximum is defined as one unit of SOD activity. MnSOD activity was determined in the presence of 5 mM sodium cyanide. CuZnSOD activity was calculated by subtracting MnSOD activity from total SOD activity.

CAT activity in solution was measured by directly monitoring the decomposition of H_2O_2 as described previously (Beers and Sizer, 1952). GPx activity was measured by an indirect assay that monitors the disappearance of NADPH (Lawrence and Burk, 1976).

Animal experiments

Athymic nude/nude mice (4–5 weeks old; Harlan Sprague Dawley Co., Madison, WI, USA) were used to study the tumorigenicity in mice. The nude mice protocol was reviewed and approved by the Animal Care and Use Facility at The University of Iowa. One million cells of each clone in 100 μl of PBS were injected into the flank region of each nude mouse. Control mice received 100 μl of PBS alone. Eight nude mice per group were used for each set of clones. Tumor size was measured with a vernier caliper twice every week and the tumor volume was calculated by the formula:

$$\text{Tumor volume}\,(\text{mm}^3) = (L \times W^2)/2$$

where L is the longest dimension of the tumor in mm and W is the shortest dimension of the tumor in mm (Zhong *et al*., 1996; Lam *et al*., 2000). When the tumors reached a predetermined volume of 1000 mm^3, animals were euthanized by CO_2 asphyxiation and this was considered the time of killing. Growth of the MnSOD-overexpressing cell lines in the athymic nude mice was evaluated up to 180 days after the injection of tumor cells.

Soft agar assay for colony formation

The effect of MnSOD transfection on the ability of PC-3 cells to form colonies in soft agar was examined to study the anchorage-independent growth of the malignant cells. Soft agar plates were prepared using a 60-mm^2 tissue culture dishes. Cells (300 or 2000) per dish were mixed in a 50 ml sterile tubes with equal volumes of 2 × Ham's F12 media containing 20% FBS and 1% agar (0.5% final). Immediately, the mixture was aliquoted in triplicate and the agar was allowed to set. The plates were incubated in a humidified chamber at 37°C for 14 days. Individual colonies of >50 cells were counted using an inverted microscope.

Cell growth

The effect of overexpression of MnSOD on cell growth was monitored by determining the number of cells as a function of time. Cells (3×10^4) were seeded onto 24-well plates in triplicate. Cells were counted every 24 h using a hemocytometer. DT was calculated from growth curve data as follows:

$$DT = 0.693 \times \frac{t_1 - t_0}{\ln (N_1/N_0)}$$

where t_0 = initial time (h), t_1 = a later time (h), N_0 = cell number at time t_0, and N_1 = cell number at time t_1 (Lam *et al*., 1997).

Cell cycle: BrdUrd labeling and flow cytometric assay

Cells were grown in 100 mm tissue culture dishes until they were 70% confluent. Cells were then pulse-labeled with 10 μM BrdUrd for 30 min at 37°C. The cells were harvested by trypsinization, washed with PBS, and fixed in 70% ethanol. Ethanol-fixed cells were stored at 4°C. The flow cytometric analysis was carried out as described previously (Menon *et al*., 2003). Briefly, the ethanol-fixed cells were washed with PBS and digested with pepsin (0.4 mg/ml in 2 M HCl) for 30 min at room temperature. After neutralization with 0.1 M-borate buffer, nuclei were separated by centrifugation at 200–400 *g* for 5 min at 4°C. Isolated nuclei were incubated with mouse anti-BrdUrd antibody (1 : 20, Beckton Dickinson Immunocytometry Systems, San Jose, CA, USA) for 1 h at room temperature. This was followed by the incubation with fluorescein isothiocyanate (FITC)-conjugated goat anti-mouse secondary antibody for an additional 1 h at room temperature. Nuclei were washed with PBS and treated with RNAase A (100 μg/ml) for 30 min, and counterstained with propidium iodide (PI: 20 μg/ml). Flow cytometric analysis was carried out on a FACScan (Becton Dickinson, San Jose, CA, USA) and data from 20 000 nuclei were recorded in list mode. The FITC fluorescence was analysed with a 535 nm band-pass filter (FL-1 channel) and PI-fluorescence was detected using a 640 nm long-pass filter (FL-3 channel). Cell cycle profile was analysed using Cellquest software.

Determination of mitochondrial membrane potential

Mitochondrial membrane potential in PC-3 cell lines was measured using two different dyes; Rh 123 (Fu *et al*., 1998) and JC-1 (Cossarizza *et al*., 1993). *Rh 123 staining:* Concentrated stock solutions of Rh 123 were prepared in 100% ethanol and stored at −20°C. Working solutions (25 μM) were prepared by diluting the stock solutions in 100% ethanol and kept on ice in the dark to minimize degradation. It has been shown that uptake of Rh 123 into mitochondria depends on mitochondrial membrane potential (Palmeira *et al*., 1996). PC-3 cell lines were incubated with 25 μM rhodamine for 30 min in F-12 medium. Cells were then washed three or four times with F-12 media without serum, trypsinized, washed and resuspended in F-12 media, and centrifuged. Cells (5×10^5) were analysed with a FACScan (Becton Dickinson, San Jose, CA, USA) equipped with a single 488 nm argon laser. *JC-1 staining:* To the cells JC-1 was added at 1 μg/ml for 10 min at 37°C. Fluorescence intensity was measured through channels FL1 at 530 nm (monomer) and FL2 at 585 nm (aggregates) using flow cytometry. The ratio between the fluorescence intensity at 585 nm (red) and another at 530 nm (green) depends on the membrane potential. At the end of the incubation period, cells were washed with PBS, trypsinized and resuspended in 500 μL PBS and analysed.

To allow elimination of the dead cells, PI (2 μg/ml) was added just before the FACS analysis.

Measurement of exogenous H_2O_2

Measurement of H_2O_2 release from PC-3 cell lines was performed as previously described (Panus *et al*., 1993). This method takes advantage of the fact that H_2O_2 reacts with HRP forming compound I, which in turn reacts with *para*-hydroxyphenyl acetic acid (pHPA) forming a stable fluorescent dimer, $[\text{pHPA}]_2$. Cell medium was removed and the cell

monolayer was washed three times with HBSS buffer. The medium was then replaced with phenol red-free HBSS (1 ml) supplemented with glucose (6.5 mM), HEPES (1 mM), sodium bicarbonate (6 mM), pHPA (1.6 mM), and HRP (95 μg/ml). The H_2O_2 was allowed to accumulate in the modified HBSS for 1 h. The released H_2O_2 was followed spectrofluorometrically by measuring the dimer formed at excitation and emission wavelengths of 323 and 400 nm, respectively. The fluorescent intensity of each sample was corrected for changes in pH and compared to standard concentrations of H_2O_2 determined by absorbance at 240 nm.

Statistical analysis

A single factor ANOVA, followed by a *post hoc* Tukey test, or Student's *t*-test was used to compare statistical differences between means. To estimate the statistical differences in growth curves, two-way ANOVA was used. To compare different groups over time for tumor volume, the linear mixed model analysis was used (Littell *et al*., 1996), assuming an auto-regressive order 1 covariance structure. In the linear mixed model, the group was considered a fixed effect and the day was considered a continuous covariate. *In vivo* survival curves were estimated by the Kaplan–Meier method with the log-rank test in order to compare groups. The linear regression analyses were carried out using Microsoft Excel™. All means were calculated from at least three experiments and error bars represent s.e.'s of the means. All activity gels and Western blots were repeated at least twice to check the reproducibility. All statistical analyses were carried out with SAS software (version 8.2) for Windows (SAS, 2001). Statistical significance was set at the 0.05 level.

Abbreviations

BrdUrd, bromodeoxyuridine; CAT, catalase; CuZnSOD, copper zinc superoxide dismutase; FBS, fetal bovine serum; GPx, glutathione peroxidase; HRP, horseradish peroxidase; JC-1, 5,5′, 6,6′-tetrachloro-1,1′,3,3′-tetraethylbenzimidazolcarbocyanine iodide|MnSOD, manganese superoxide dismutase; PBS, phosphate-buffered saline; pHPA, *para*-hydroxy phenyl acetic acid; PI, propidium iodide; Rh 123, rhodamine 123.

Acknowledgements

We thank Dr Fredrick Domann, Dr Freya Schafer, and Sean Martin for their helpful discussions. We thank Dr Douglas Spitz for his help with antioxidant enzyme measurements. We also thank Dr Hong P Wang, Susan Walsh, and Sarita Menon for their various help; Justin Fishbaugh in the Flow Cytometry Core Facility for his help with flow techniques; and Ms Kellie Bodeker for her editorial assistance. This work was supported by NIH Grants CA 81090 and CA66081.

References

Allen RG and Balin AK. (1989). *Free Radic. Biol. Med.*, **6,** 631–661.

Antunes F and Cadenas E. (2000). *FEBS Lett.*, **475,** 121–126.

Bae VL, Jackson-Cook CK, Brothman AR, Maygarden SJ and Ware JL. (1994). *Int. J. Cancer*, **58,** 721–729.

Bae VL, Jackson-Cook CK, Maygarden SJ, Plymate SR, Chen J and Ware JL. (1998). *Prostate*, **34,** 275–282.

Bae YS, Kang SW, Seo MS, Baines IC, Tekle E, Chock PB and Rhee SG. (1997). *J. Biol. Chem.*, **272,** 217–221.

Barnouin K, Dubuisson ML, Child ES, Fernandez de Mattos S, Glassford J, Medema RH, Mann DJ and Lam EW. (2002). *J. Biol. Chem.*, **277,** 13761–13770.

Beauchamp C and Fridovich I. (1971). *Anal. Biochem.*, **44,** 276–287.

Beers Jr RF and Sizer IW. (1952). *J. Biol. Chem.*, **195,** 133–140.

Cerutti PA. (1985). *Science*, **227,** 375–381.

Chance B, Sies H and Boveris A. (1979). *Physiol. Rev.*, **59,** 527–605.

Chen Q, Fischer A, Reagan JD, Yan LJ and Ames BN. (1995a). *Proc. Natl. Acad. Sci. USA*, **92,** 4337–4341.

Chen Q, Olashaw N and Wu J. (1995b). *J. Biol. Chem.*, **270,** 28499–28502.

Chen QM, Bartholomew JC, Campisi J, Acosta M, Reagan JD and Ames BN. (1998). *Biochem. J.*, **332** (Part 1)**,** 43–50.

Chen QM, Liu J and Merrett JB. (2000). *Biochem. J.*, **347,** 543–551.

Chin CW, Foss AJ, Stevens A and Lowe J. (2003). *J. Pathol.*, **200,** 308–313.

Church SL, Grant JW, Ridnour LA, Oberley LW, Swanson PE, Meltzer PS and Trent JM. (1993). *Proc. Natl. Acad. Sci. USA*, **90,** 3113–3117.

Cossarizza A, Baccarani-Contri M, Kalashnikova G and Franceschi C. (1993). *Biochem. Biophys. Res. Commun.*, **197,** 40–45.

da Silva MM, Sartori A, Belisle E and Kowaltowski AJ. (2003). *Am. J. Physiol. Heart Circ. Physiol.*, **285,** H154–H162.

Foster CS, Cornford P, Forsyth L, Djamgoz MB and Ke Y. (1999). *BJU Int.*, **83,** 171–194.

Fu W, Luo H, Parthasarathy S and Mattson MP. (1998). *Neurobiol. Dis.*, **5,** 229–243.

Jung K, Seidel B, Rudolph B, Lein M, Cronauer MV, Henke W, Hampel G, Schnorr D and Loening SA. (1997). *Free Radic. Biol. Med.*, **23,** 127–133.

Klaunig JE, Xu Y, Isenberg JS, Bachowski S, Kolaja KL, Jiang J, Stevenson DE and Walborg Jr EF. (1998). *Environ. Health. Persp.*, **106** (Suppl 1)**,** 289–295.

Lam EW, Hammad HM, Zwacka R, Darby CJ, Baumgardner KR, Davidson BL, Oberley TD, Engelhardt JF and Oberley LW. (2000). *J. Dent. Res.*, **79,** 1410–1417.

Lam EW, Zwacka R, Engelhardt JF, Davidson BL, Domann Jr FE, Yan T and Oberley LW. (1997). *Cancer Res.*, **57,** 5550–5556.

Lawrence RA and Burk RF. (1976). *Biochem. Biophys. Res. Commun.*, **71,** 952–958.

Li JJ, Oberley LW, Fan M and Colburn NH. (1998a). *FASEB J.*, **12,** 1713–1723.

Li N, Oberley TD, Oberley LW and Zhong W. (1998b). *J. Cell. Physiol.*, **175,** 359–369.

Li N, Oberley TD, Oberley LW and Zhong W. (1998c). *Prostate*, **35,** 221–233.

Li S, Yan T, Yang JQ, Oberley TD and Oberley LW. (2000). *Cancer Res.*, **60,** 3927–3939.

Liochev SI and Fridovich I. (1997). *Free Radic. Biol. Med.*, **23,** 668–671.

Littell RC, Milliken GA, Stroup WW and Wolfinger RD. (1996). *SAS System for Mixed Models*. SAS Institute Inc.: Cary, NC.

Liu R, Oberley TD and Oberley LW. (1997). *Hum. Gene. Ther.*, **8,** 585–595.

Menon SG, Sarsour EH, Spitz DR, Higashikubo R, Sturm M, Zhang H and Goswami PC. (2003). *Cancer Res.*, **63,** 2109–2117.

Monteiro HP and Stern A. (1996). *Free Radic. Biol. Med.*, **21,** 323–333.
Murrell GA, Francis MJ and Bromley L. (1990). *Biochem. J.*, **265,** 659–665.
Oberley LW and Buettner GR. (1979). *Cancer Res.*, **39,** 1141–1149.
Oberley LW and Oberley TD. (1986). *Free Radicals, Aging, and Degenerative Disease, Modern Aging Research* , Vol. 8. Johnson Jr JE, Walford R, Harmon D and Miquel J (eds). Alan R. Liss: New York, pp. 352–371.
Oberley LW and Spitz DR. (1985). *CRC Handbook of Methods for Oxygen Radical Research*, Greenwald Ra (ed). CRC Press: Boca Raton, FL, pp. 217–220.
Oberley TD, Allen RG, Schultz JL and Lauchner LJ. (1991). *Free. Radic. Biol. Med.*, **10,** 79–83.
Orr WC and Sohal RS. (1994). *Science*, **263,** 1128–1130.
Palazzotti B, Pani G, Colavitti R, De Leo ME, Bedogni B, Borrello S and Galeotti T. (1999). *Int. J. Cancer*, **82,** 145–150.
Palmeira CM, Moreno AJ, Madeira VM and Wallace KB. (1996). *J. Pharmacol. Toxicol. Methods*, **35,** 35–43.
Panus PC, Radi R, Chumley PH, Lillard RH and Freeman BA. (1993). *Free Radic. Biol. Med.*, **14,** 217–223.
Reers M, Smith TW and Chen LB. (1991). *Biochemistry*, **30,** 4480–4486.
Rodriguez AM, Carrico PM, Mazurkiewicz JE and Melendez JA. (2000). *Free Radic. Biol. Med.*, **29,** 801–813.
SAS system for windows® (2001) Version 8.2 SAS Institute: Cary, NC.
Schafer FQ and Buettner GR. (2001). *Free Radic. Biol. Med.*, **30,** 1191–1212.
Schreck R, Rieber P and Baeuerle PA. (1991). *EMBO J.*, **10,** 2247–2258.
Sun Y. (1990). *Free Radic. Biol. Med.*, **8,** 583–599.
Suzukawa K, Miura K, Mitsushita J, Resau J, Hirose K, Crystal R and Kamata T. (2000). *J. Biol. Chem.*, **275,** 13175–13178.
Wang D, Li S, Au W, Cui H and Yang X. (1997). *Chin. Med. Sci. J.*, **12,** 76–79.
Weydert C, Roling B, Liu J, Hinkhouse MM, Ritchie JM, Oberley LW and Cullen JJ. (2003). *Mol. Cancer Ther.*, **2,** 361–369.
Zhang HJ, Yan T, Oberley TD and Oberley LW. (1999). *Cancer Res.*, **59,** 6276–6283.
Zhang HJ, Zhao W, Venkataraman S, Robbins ME, Buettner GR, Kregel KC and Oberley LW. (2002a). *J. Biol. Chem.*, **277,** 20919–20926.
Zhang Y, Zhao W, Zhang HJ, Domann FE and Oberley LW. (2002b). *Cancer Res.*, **62,** 1205–1212.
Zhong W, Oberley LW, Oberley TD, Yan T, Domann FE and St Clair DK. (1996). *Cell Growth Differ.*, **7,** 1175–1186.